EUROPHYSICS LETTERS 15 November 1992

Europhys. Lett., **20** (6), pp. 499-504 (1992)

Matrix-Modulated Swelling of a Polymer Brush.

A. BUDKOWSKI (*) (§), U. STEINER (*), J. KLEIN (*) and L. J. FETTERS (**)

(*) *Department of Materials and Interfaces, Weizmann Institute of Science Rehovot 76100, Israel*

(**) *Exxon Research and Engineering Corp., Corporate Research Laboratories Annandale, NJ 08801, USA*

(received 13 May 1992; accepted in final form 10 September 1992)

PACS. 36.20 – Macromolecules and polymer molecules.
PACS. 68.22 – Surface diffusion, segregation and interfacial compound formation.

Abstract. – We have measured, using nuclear-reaction analysis, the concentration depth profiles of polymer brushes consisting of end-tethered deuterated polystyrene tails within a polystyrene homopolymer, as a function of the surface coverage σ of tails and of the degree of polymerisation P of the polymer matrix. We find that the onset of brush swelling is shifted to higher σ values at higher P as expected from theory. Within the range of our parameters the $L(\sigma)$ and $L(P)$ variations are consistent with predictions of scaling and mean-field models, where L is the effective brush thickness.

Flexible chains that are densely attached by one end only at a solid-liquid interface are known as polymeric brushes [1]; they are used as surface modifiers in a wide range of applications. Such grafted layers have structures that are very different to those of adsorbed chains (where segments along the entire chain contour may attach at the interface): in particular, for the case of densely grafted polymer chains in a good-solvent medium, where the mean interanchor spacing $s < R_0$, the polymer coil size, the chains will be stretched normal to the substrate and the brush thickness L is predicted [1,2] to vary as

$$L = \text{const}\, N a \sigma^{1/3} . \tag{1}$$

Here N is the degree of polymerisation of the chains, a is a monomer size, and the surface coverage $\sigma = a^2/s^2$. Equation (1) has been demonstrated experimentally in a number of studies for the case of polymer brushes in good solvents, using force measurement techniques [3,4], small-angle neutron scattering [5], and most recently neutron reflectometry [6]. The end-groups tethering the polymer chains to the surfaces can be covalently bonding chemical groups [5], physically adhering functional groups [3], or an adsorbing polymeric moiety anchoring a nonadsorbing one [3,4], as in diblock copolymers.

The basic physical reason for the strong stretching of chains within the brush is as follows [2]: in a good solvent, segments from neighbouring chains tend to avoid each other due to excluded-volume effects. This acts to stretch the chains away from the surface, a

(§) On leave of absence from Jagellonian University of Cracow, Poland.

tendency which is resisted by entropic (elastic) restoring forces. Equation (1) represents the layer thickness minimising the overall free energy for a given value of σ [2]. A particularly interesting situation arises when the liquid matrix is not a low-molecular-weight fluid but is itself polymeric with degree of polymerisation P, say. One then expects that for $P > N^{1/2}$ the excluded-volume interactions become progressively screened out, and the stretching of chains within a polymeric brush will be modulated by the value of P itself. This situation has been considered theoretically [7-11], using both scaling [7, 8, 10] and self-consistent mean-field [9, 11] approaches, by a number of workers; different regimes of brush structure in the (P, σ)-plane, each with its appropriate scaling law, can be classified [7, 9]. These include the case of low surface coverage by the tethered chains, such that $s > R_0$, where one has nonoverlapping coils on the surface; at much higher σ values the coils stretch normal to the surface as described. For the case of a solvent ($P \ll N^{1/2}$) this occurs in accordance with eq. (1); in the regime $N > P > N^{1/2}$, however, the P-mer matrix chains may penetrate the brush («wet-brush» regime) to screen the excluded-volume interactions, as noted; in this case the brush thickness is predicted [7-9] to vary as

$$L = \text{const}\, NaP^{-1/3}\sigma^{1/3} \qquad (N > P > N^{1/2}). \tag{2}$$

At high values of the surface coverage by the tethered N-mer, progressive exclusion of the P-mer matrix chains from within the brush layer occurs (leading to the so-called «dry-brush» regime). Moreover, at high values of P ($P \geqslant N$) complete exclusion of the P-mers from within the brush is predicted [7-9]; in this case the transition as σ increases is expected to cross from a regime of nonoverlapping tethered N-mers, through an overlapping but screened (nonswollen) regime, to a swollen dry-brush regime (no matrix chains within the brush layer).

In contrast to the case of surface-tethered polymers in simple solvents [3-6], there have been few experimental studies of brushes in polymeric matrices [12, 13]. We report here the first systematic investigation of how the thickness L of a polymeric N-mer brush in a P-mer matrix varies as a function of P and σ. In our experiments we use a highly asymmetric polyisoprene (PI)-deuterated polystyrene (dPS) diblock copolymer, which is attached by its short PI moiety to the polymer-air interface of a thin polystyrene (PS) film of different molecular weights (the P-mer matrix). The molecular characteristics of the polymers used in our experiments are given in table I. Both the thickness of the dPS brush layer and the total surface excess σ of the deuterated brush at the homopolymer-air interface are determined using Nuclear Reaction Analysis (NRA), based on the reaction $^3\text{He} + {}^2\text{H} \rightarrow {}^4\text{H} + {}^1\text{H} + 18.35\,\text{MeV}$, as described in detail earlier [14].

Thin films (thickness ~ 500 nm) of the PS homopolymer containing different volume

TABLE I. – *Molecular weights and polydispersities (expressed as the ratio of weight-to-number average) of samples used in this study.*

Polymer	M_w [a]	M_w/M_n [b]
PS(9.2 k)	9 200	1.03
PS(51.5 k)	51 500	1.04
PS(330 k)	330 000	1.04
PI-dPS	PI = 10 300 [b]	1.03
	dPS = 100 000	1.03

([a]) Via low-angle laser light scattering.
([b]) Via size exclusion chromatography.

fractions of the PI-dPS diblock were spin cast onto polished silicon substrates from toluene solution, and sealed under vacuum (10^{-5} Torr) in glass ampoules. Samples were annealed at 180 °C for one day, and it was checked that this time sufficed for equilibrium behaviour to be attained. The volume fraction ($\phi(z)$) *vs.* depth (z) profile of the PI-dPS within the sample is measured using NRA [14] at an incident ^{3}He beam energy of 700 keV, the absolute values of ϕ being determined by comparison with the known total diblock content of the film. The resolution of NRA in depth profiling near the sample surface depends on the precise conditions (incident energies, scattering angles) used; this resolution $\partial(\sim (8 \div 9)$ nm HWHM in the present study) was explicitly determined by profiling of unannealed films for each experimental run.

Typical profiles before and after annealing of the films are shown on the left-hand side of fig. 1(*a*)-*c*)). These show how the PI-dPS concentration within each layer varies with depth from the polymer surface. The presence of the peak shows clearly, on annealing, that the PI-dPS diblock migrates to the polymer-air interface. The possibility that micelles with a PI core and a dPS corona are formed, and that they migrate to the PS homopolymer-air interface due to the lower surface energy of the dPS—as observed earlier for dPS-poly(vinyl pyridine) diblocks in a PS matrix [15]—was carefully investigated: electron microscopy of PS films containing the diblock and annealed in the conditions of the experiments failed to reveal any evidence of micellar formation after staining with OsO_4, even at 15% concentration of the PI-dPS in the highest-molecular-weight homopolymer, PS(330k). In another control

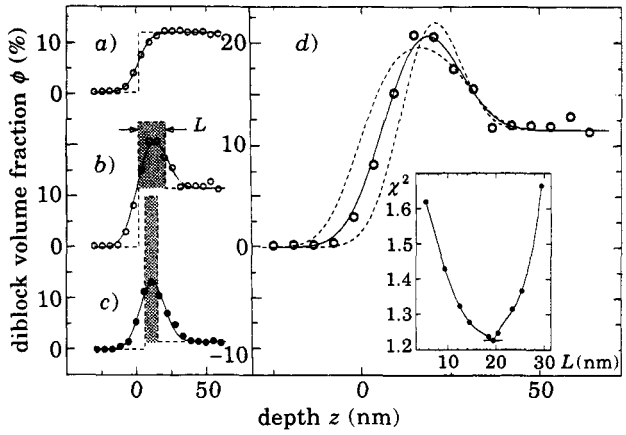

Fig. 1. – *a*) Concentration-depth profile of an unannealed thin film of PS(9.2k) containing 12% volume fraction of PI-dPS on silicon wafer, near the polymer-air interface ($z = 0$). The solid line is a convolution of the step function at $z = 0$ (broken line) with the system resolution $\partial = 9.1$ nm (HWHM). *b*) As *a*), following 24 h annealing at 180 °C. The solid curve is a convolution of the top-hat–like distribution represented by the broken line, with the system resolution ∂. The shaded area corresponds to the measured surface excess of the diblock. *c*) Concentration-depth profile near the polymer-air interface of a PS(330k) film containing the PI-dPS diblock following annealing at 180 °C for 24 h. The initial volume fraction of the diblock in the as-cast film was 3%, but after build-up of the surface peak this dropped (as shown) to a value $\phi_b = 1.5\%$. The solid curve is the convolution of the top-hat–like distribution (broken curve) with ∂. The shaded area equals the measured surface excess of the diblock. *d*) Convolution of step functions of different widths L and volume fraction ϕ_m (keeping $L\phi_m$ constant and equal to the surface excess, as described in the text) with ∂. The data corresponds to fig. 1*b*). Broken lines are for $L = 10$ and 30 nm, respectively. (The profiles have been shifted for clarity to superpose on their r.h.s.) The inset shows the variation of the fit parameter χ^2 (mean square of residuals) with L. The best fit ($L = 19.4$ nm) corresponds to the sharp minimum in χ^2, and was used to generate the solid line of the profile (the error of $\pm$ 2 nm shown as a horizontal bar in the inset is the estimated uncertainty in the value of L corresponding to the minimum in χ^2).

experiment to simulate the effect of hypothetical dPS coronas in the PS homopolymer, we annealed thin films of PS(330k) containing 15% of a high-molecular-weight dPS homopolymer ($M_w = 1.9 \cdot 10^6$) at 180 °C for three days: there was no evidence over this time of any aggregation of the dPS at the polymer-air interface. Similarly, dPS homopolymer with molecular weight ($M_w = 1.04 \cdot 10^5$) similar to the dPS moiety of the copolymer showed no sign of segregating to the air interface when incorporated into the PS(330k) film and annealed in similar conditions. These observations suggest that no micelles are forming in the conditions of our experiments, as is also consistent with calculations [15] for this system using the appropriate PI-PS segmental interaction parameter [16]; they also show unequivocally that the surface excess of dPS at the polymer-air interface determined by NRA (fig. 1*b*) and *c*)) is driven solely by the segregation of the PI moieties to the polymer-air interface (1), with the dPS tails dangling into the PS homopolymer.

The basic concentration *vs.* depth profiles (as in fig. 1) obtained from the NRA measurements can yield the specific surface coverage by the dPS tails, $\sigma = a^2/s^2$, where a is taken as a statistical segment length for PS. σ is related to the volume fraction excess Γ as

$$\sigma = \frac{\Gamma}{N_c a} = \frac{1}{N_c a} \int_0^{z_b} (\phi(z) - \phi_b)\, dz , \tag{3}$$

where ϕ_b in the bulk copolymer volume fraction at depth z_b and N_c is its degree of polymerisation. σ could be varied by varying the bulk concentration of the diblock within the homopolymer, in an appropriate manner, in the different PS matrices. For example, the profiles shown in fig. 1*b*) and *c*) are for identical values of the surfaces excess σ ($3.7 \cdot 10^{-3}$) of the dPS tails, obtained for the PS(9.2k) and PS(330k) homopolymer matrices by adjusting the bulk concentration in the films to yield final ϕ_b values of 11.5% and 1.5%, respectively.

The resolution ∂ of the NRA technique is comparable with the characteristic unperturbed dimension of the dPS moiety (for which the diameter of gyration $2R_g = 16.4$ nm). This precludes any detailed determination of the brush segment density profile (for example, any distinction between parabolic or other types of profile). It is, however, possible from the $\phi(z)$ profile to obtain an explicit measure of the brush thickness normal to the polymer-air interface. We do this by assuming the brush to have a uniform volume fraction ϕ_m over a width L (2). Then the product $L\phi_m$ is fixed by the measured surface excess per unit area,

$$\Gamma = L\phi_m . \tag{4}$$

The step function [L, ϕ_m] is convoluted with the known NRA resolution ∂ to yield a broadened surface peak, which is then fitted to the experimental profile. This procedure is illustrated in fig. 1: profiles such as fig. 1*a*) enable ∂ to be extracted for any given experimental run. Subsequent profiles within the run are fitted to a top-hat brush profile by convoluting with this experimental resolution, varying L and ϕ_m subject to the condition of eq. (4). Figure 1*b*) and *c*) show the top-hat distributions (broken lines) together with the convoluted profiles (solid curves) which best fit the data. Figure 1*d*) shows that, within the experimental scatter, a unique width L can be extracted for the top-hat brush profile corresponding to the experimentally measured profile.

---

(1) We note that the polymer-air interface, to be continuously covered by a polyisoprene melt layer one monomer thick, requires values $\sigma \approx 10^{-2}$ in our experiments.

(2) The self-consistent mean-field models [9, 11], which yield a parabolic segment density profile for the brush (for a recent review see, *e.g.*, [17]), predict the same scaling and brush regime behavior as do the scaling models [7, 8] where a top-hat distribution is assumed.

The variation of the brush width L thus determined with surface excess σ is shown in fig. 2 on a double logarithmic plot for the PS(9.2k) and PS(330k) homopolymer matrices (the variation of $L(\sigma)$ for the PS(51.5k) matrix is intermediate between these, and—with the exception of one point, see later—is omitted for clarity). Both sets of data approach, at low coverage, a value of L which is close to R_g. With increase in the surface coverage, the brush width L increases in a manner which depends on the degree of polymerisation P of the host PS homopolymer. For the lower-molecular-weight matrix, PS(9.2k), we are in the «wet-brush» regime $N > P > N^{1/2}$. The predicted variation $L \sim \sigma^{1/3}$ for this regime is shown as a broken line in fig. 2; the data (open circles) is scattered but is consistent with this variation.

The $L(\sigma)$ data for the PS(330k) matrix (solid circles) are rather different. We note especially that for this higher P matrix the surface coverage at which swelling of the brush commences is significantly higher than for the PS(9.2k) matrix. This implies that over the range $10^{-3} < \sigma < 5 \cdot 10^{-3}$ the brush is in the screened (nonswollen) regime [7, 9]; for $\sigma > 4 \cdot 10^{-3}$ the data can be fitted by an apparent power law (solid line in fig. 2)

$$L \sim \sigma^q, \qquad q = 0.54 \pm 0.06.$$

If, as has been predicted [7-9], the nonswollen regime, $L \sim \sigma^0$, for this high-molecular-weight matrix reverts at higher σ values rapidly to a dry-brush situation $L \sim \sigma$ (expelling the P chains from within the grafted layer), then the intermediate value of the apparent exponent q may indicate a transition region.

It is instructive to examine directly the variation with σ of the mean concentration ϕ_m of tails within the brush and this is done in fig. 3 for the PS(9.2k) and PS(330k) matrices. The

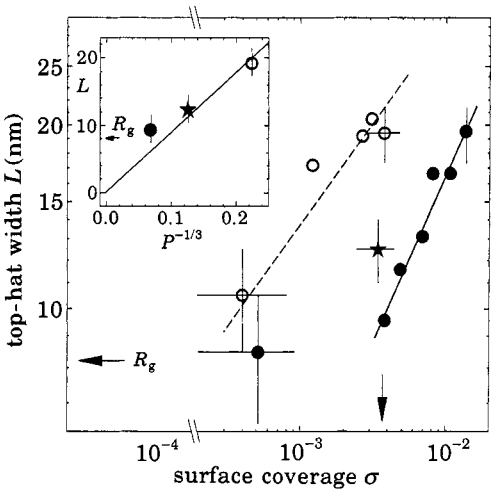

Fig. 2.

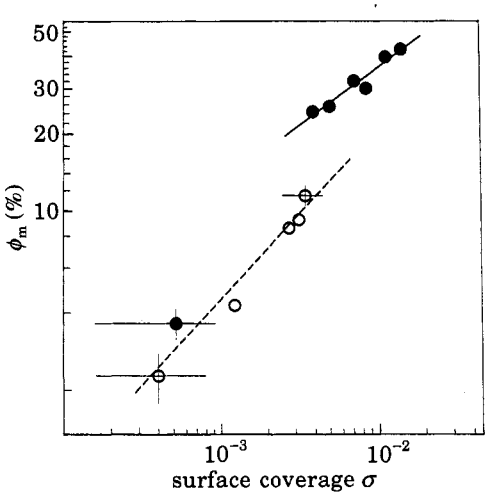

Fig. 3.

Fig. 2. – Variation of the width L of the best-fit top-hat distribution (see fig. 1) with surface coverage σ, for host matrices: ○ PS(9.2k), ● PSD(330k), and ★ PS(51.5k). The broken line corresponds to $L \sim \sigma^{1/3}$, while the solid line corresponds to $L \sim \sigma^{0.54}$ as described in the text. The inset shows how L varies with $P^{-1/3}$ for the equi-σ situation (arrow in the main figure) ($\sigma = 3.7 \cdot 10^{-3}$).

Fig. 3. – Variation of the volume fraction of the best-fit top-hat brush distributions as in fig. 1, ϕ_m (normalised to the units of dPS fraction), with surface coverage σ. ○ host matrix PS(9.2k); ● host matrix PS(330k). The broken and solid lines correspond to power law variations $\phi_m \sim \sigma^{2/3}$ and $\phi_m \sim \sigma^{0.46}$ (complementary to the solid line in fig. 2), respectively.

broken line is the predicted variation $\phi_m \sim \sigma^{2/3}$ of the mean volume fraction of brush segments within a layer of thickness L in the wet-brush regime (from eq. (2)), while the solid line is the best-fit power law complementary to fig. 2; it is seen more clearly, however, that—for the PS(330k) matrix—even at the highest σ value, ϕ_m (at ca. 50%) has still not attained the dry-brush limit (100%), consistent with the transition regime noted above.

Finally, it is of interest to compare directly the variation of the brush thickness L with P, as predicted by eq. (2), with our data. By suitable adjustment of the diblock concentration within the homopolymer films, to values $\phi_b = 1.5\%$, 2.1% and 11.5% in the PS(330k), PS(51.5k) and PS(9.2k) homopolymers, respectively, we were able to achieve an equi-σ situation ($\sigma = (3.7 \pm 0.2) \cdot 10^{-3}$, see arrow in fig. 2) for the brush in the three matrices. The inset to fig. 2 shows the variation of L with $P^{-1/3}$ for this constant σ value: the straight line is the variation expected from eq. (2) for wet brushes. The data, while limited, is again consistent with the theoretical prediction.

In summary, we have presented systematic data on the structure of polymer brushes attached by one end at a polymer-air interface for different surface densities and different molecular weights of the homopolymer matrix. Within the range of our experimental parameters, our results are in accord with expectations based on theoretical models of end-attached chains in polymeric matrices.

* * *

We thank the German-Israel Foundation (GIF) and the US-Israel Binational Science Foundation (BSF) for support of this work.

REFERENCES

[1] DE GENNES P. G., *Adv. Colloid Interface Sci.*, **27** (1987) 189.
[2] ALEXANDER S., *J. Phys. (Paris)*, **38** (1977) 983.
[3] TAUNTON H. J., TOPRAKCIOGLU C., FETTERS L. J. and KLEIN J., *Nature (London)*, **332** (1988) 712; *Macromolecules*, **23** (1990) 571.
[4] HALPERIN A., TIRRELL M. and LODGE T., *Adv. Polymer Sci.*, **100** (1991) 31.
[5] AUROY P., AUVRAY L. and LEGER L., *Phys. Rev. Lett.*, **66** (1991) 719.
[6] FIELD J. B., TOPRAKCIOGLU C., BALL R. C., STANLEY H. B., DAI L., BARFORD W., PENFOLD J., SMITH G. and HAMILTON W., *Macromolecules*, **25** (1992) 434.
[7] DE GENNES P. G., *Macromolecules*, **13** (1980) 1069.
[8] LEIBLER L., *Macromol. Chem. Macromol. Symp.*, **16** (1988) 1.
[9] ZHULINA E. B., BORISOV O. V. and BROMBACHER L., *Macromolecules*, **24** (1991) 4679.
[10] MARQUES C., JOANNY J. F. and LEIBLER L., *Macromolecules*, **21** (1988) 1051.
[11] SHULL K. R., *J. Chem. Phys.*, **94** (1991) 5723.
[12] JONES R. A. L., KRAMER E. J., NORTON L. J., SHULL K. R., FELCHER G. P., KARIM A. and FETTERS L. J., preprint.
[13] ZHAO X., ZHAO W., RAFAILOVICH M. H., SOKOLOV J., RUSSELL T. P., KUMAR S. K., SCHWARZ S. A. and WIKIENS B. J., *Europhys. Lett.*, **15** (1991) 725.
[14] CHATURVEDI U. K., STEINER U., ZAK O., KRAUSCH G., SCHATZ G. and KLEIN J., *Phys. Rev. Lett.*, **63** (1989) 616; *Appl. Phys. Lett.*, **56** (1990) 1228.
[15] SHULL K. R., WINEY K. I., THOMAS E. L. and KRAMER E. J., *Macromolecules*, **24** (1991) 2748.
[16] TANAKA H. and HASHIMOTO T., *Macromolecules*, **24** (1991) 5398.
[17] WITTEN T., *Macromol. Rep. A*, **29** (1992) 87.